International Journal of Engineering Research and Development

DOI: 10.29137/ijerad.1444519

Volume:17 Issue:1 Pages:55-64 March/2025

Research Article

LiDAR Based SLAM: A Comparative Evaluation with LeGO-LOAM and HDL-Graph SLAM

Yiğit Çağatay Kuyu[1], Fahri Vatansever[2*]

[1]Karsan Automotive, TURKIYE
[2]Bursa Uludağ University, TURKIYE

***Received**: 28/02/2024 **Accepted**:5/7/2024 **Published Online:** 15/03/2025*
***Final Version**: 01/03/2025*

Abstract

Simultaneous localization and mapping (SLAM) is an area of research that is experiencing rapid advancements, with a significant impact on improving the navigation and perception capabilities of vehicles, thereby enabling their safe operation in complex environments. This study presents a comprehensive overview of the recent developments in SLAM and conducts a comparative evaluation of two widely employed SLAM methods. The evaluation is based on rigorous performance analysis using the KITTI dataset, which is one of the most popular benchmark datasets for evaluating SLAM algorithms. The evaluation focuses on two essential metrics: absolute trajectory error (ATE) and relative pose error (RPE), which provides valuable insights into the accuracy and consistency of pose estimation over time. By quantifying the deviation between estimated trajectories and ground truth data, ATE sheds light on the global accuracy of the SLAM system, while RPE examines the local error and the system's ability to maintain reliable pose estimates within sequential frames. A thorough discussion is provided on the advantages, distinctive features, and performance characteristics of each technique, thereby offering valuable insights to propel future research in this area.

Key Words

"SLAM, LiDAR, LeGO-LOAM, HDL-Graph SLAM"

**** Corresponding Author:** fahriv@uludag.edu.tr*

1. Introduction

Technological developments, which are evident in every field, are also experienced in robotic system applications. One of the most important properties of these systems is their ability to operate autonomously (without continuous human supervision or remote control). This requires the execution of many different processes together for autonomous mobile robotic systems (Figure 1) (Makarenko et al., 2002; Kudriashov et al., 2020).

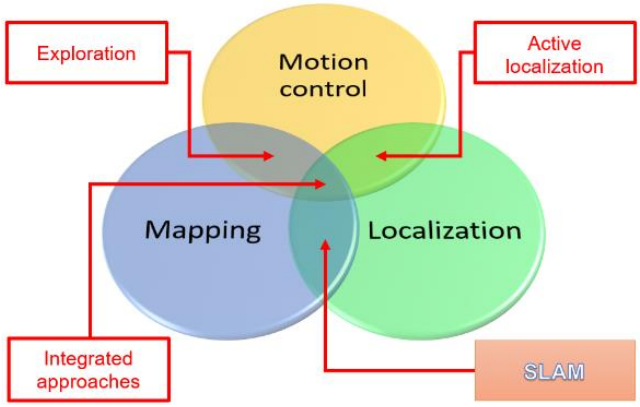

Figure 1. The fields of mobile robotic Systems

Simultaneous localization and mapping (SLAM) technology, originally proposed by Smith in 1986 (Smith & Cheeseman, 1986), has found widespread applications in diverse fields such as autonomous robots (ARs) (Kim & Eustice, 2013; Kim et al., 2018) and autonomous vehicles (AVs) (Takleh et al., 2018; Gao et al., 2020). SLAM aims to solve the challenging task of simultaneously mapping an unknown environment and accurately localizing the sensor system within it, utilizing the signals provided by the sensors. In the realm of robotics and AVs, mapping plays a pivotal role as it enables the identification and visualization of key landmarks, facilitating a comprehensive understanding of the environment. Additionally, the generated map aids in state estimation, enabling reliable localization and minimizing estimation errors when revisiting registered areas (Guclu & Can, 2019; Hoshi et al., 2022).

The field of SLAM encompasses a diverse range of sensor-based methods, with Light Detection and Ranging (LiDAR) SLAM and Visual SLAM (V-SLAM) standing out as two prominent categories. LiDAR-SLAM relies on LiDAR sensors to capture precise geometric information about the environment, while V-SLAM leverages cameras as primary sensors, extracting valuable visual information from images (Cheng et al., 2022). V-SLAM offers the provision of rich information, cost-effectiveness, lightweight design, and compact size. However, it encounters challenges when operating in scenarios characterized by unstable ambient lighting conditions and limited surface texture, particularly in outdoor environments (Zhang & Zhang, 2022).

On the other hand, LiDAR-SLAM leverages the inherent advantages of LiDAR technology, wherein the acquired point cloud data directly represents the geometric relationships within the environment. This characteristic makes LiDAR-SLAM particularly suitable for tasks such as path planning and vehicle navigation. Notably, LiDAR-SLAM is unaffected by lighting conditions and provides high-ranging accuracy, enhancing its performance in various environmental settings (Niloy et al., 2021). The selection between LiDAR-SLAM and V-SLAM depends on the specific requirements of the application and the prevailing environmental conditions. While V-SLAM excels in capturing rich visual information and offers cost-effectiveness, its performance may be hindered by factors such as lighting variations and texture limitations.

Also, LiDAR-SLAM provides reliable geometric information and robust performance irrespective of lighting conditions, albeit at potentially higher costs and complex hardware requirements. Hence, comprehending the strengths and limitations of both approaches is crucial for selecting the most appropriate SLAM method for a given application (Cheng et al., 2022; Huang, 2021). The advancement of SLAM algorithms has garnered significant attention, with researchers making notable progress in their development over the past few decades. In 1991, the probabilistic approach was employed to develop the SLAM technique based on the earlier work conducted in (Smith & Cheeseman, 1986), introducing the implementation of the Extended Kalman Filter (EKF) method (Leonard & Durrant-Whyte, 1991).

In 2001, a pioneering utilization of Millimeter Waves (MMW) to construct relative maps, focusing on the environment mapping process of mobile robots, was introduced (Dissanayake et al., 2001). The year 2002 witnessed the emergence of the Fast-SLAM algorithm, which integrates Extended Kalman Filter (EKF) techniques and particle filters for addressing non-Gaussian non-linear systems. By partitioning the conditional map and motion model components, this method curtails the sampling space and reduces the dimensionality of the state space (Montemerlo et al., 2002). A seminal advancement in SLAM techniques emerged in 2004 with Rat-

SLAM, a modern approach amalgamating path integration, visual association, and competitive attractor processes to achieve robust and comprehensive SLAM (Milford et al., 2004).

In the trajectory of SLAM evolution, the year 2006 introduced the Square Root Smoothing and Mapping (SAM) technique, leveraging square root information smoothing to enhance mapping efficiency (Dellaert & Kaess, 2006). The ensuing year, 2008, marked the introduction of UFastSLAM, a robust algorithm founded on scale unscented transformation (Kim et al., 2007). The year 2009 saw the introduction of the Differential Evolution technique to tackle SLAM challenges (Moreno et al., 2009).

Transitioning into the 2010s, this progression culminated in the extension of incremental smoothing and mapping (iSAM), geared towards facilitating online multi-robot mapping through multiple pose graphs (Kim et al., 2010). In 2012, iSAM2 emerged, leveraging nonlinear optimization and incremental filters (Kaess et al., 2011). The realm of visual SLAM saw the inception of ORB-SLAM in 2015 (Mur-Artal et al., 2015), followed by its advancements in 2017 with ORB-SLAM2 (Mur-Artal & Tardós, 2017) and in 2021 with ORB-SLAM3 (Campos et al., 2021), collectively contributing to the resolution of SLAM complexities.

Concurrently, driven by the decreasing cost of LiDAR technology and the safety imperatives of autonomous driving, the past decade has witnessed the inception of remarkable LiDAR SLAM algorithms. In 2014, the real-time LOAM method was unveiled, distinguished by its bifurcated approach wherein one algorithm handles high-frequency, low-fidelity odometry estimation, while the other addresses fine-grained point cloud matching and registration (Zhang & Singh, 2014). This trajectory was augmented with the formulation of V-SLAM, a framework amalgamating visual and LiDAR odometry to establish point cloud registrations and ego-motion estimations (Zhang & Singh, 2015).

The year 2018 introduced LeGO-LOAM, a lightweight and ground-optimized LiDAR odometry and mapping approach catering to real-time six-degree-of-freedom pose estimation, capitalizing on ground plane segmentation and optimization (Shan & Englot, 2018). Building upon this, the subsequent year saw the inception of HDL-Graph SLAM, founded on a graph-based paradigm and anchored by NDT scan matching-based odometry estimation and loop detection (Koide et al., 2019).

The evolution of SLAM methodologies has been a focal point of rigorous investigation spanning numerous global institutions. In this vein, this paper assumes a pivotal role by furnishing a comprehensive comparative analysis between two prominent LiDAR-based SLAM algorithms, namely LeGO-LOAM and HDL-Graph SLAM, both of which have attained open-source status. This study further delves into an incisive exploration of the performance characteristics inherent in each algorithm, undertaken within the context of the widely adopted KITTI dataset (KITTI Dataset, 2023), predicated upon the metrics of Absolute Trajectory Error (ATE) and Relative Positional Error (RPE) (Sturm et al., 2012). Such meticulous scrutiny assumes paramount significance, as it affords a discerning grasp of the intrinsic attributes, merits, and demerits underpinning each algorithmic instantiation.

This paper is organized as follows: The compared/used algorithms and used error metrics are explained in Section 2. The experimental results are given in Section 3 and Section 4 includes conclusions.

2. Materials and Methods

SLAM, which is basically about building a map of an unknown environment with a mobile robot and navigating the robot using this map, can be applied in 2D and 3D. (Figure 2).

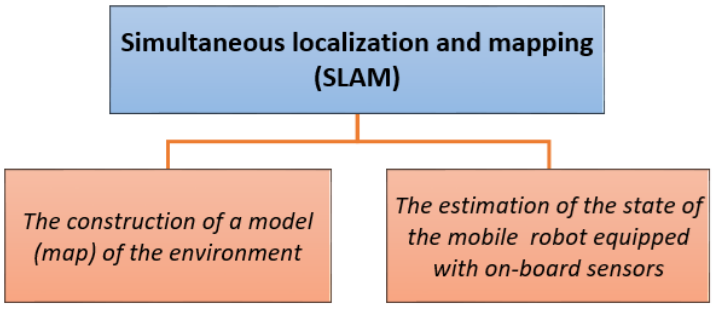

Figure 2. The main consists of SLAM

SLAM system, which includes two main components consists of multiple processes (data association, landmark extraction, state estimation and update, landmark update etc.): the front-end and the back-end. Here, the front-end abstracts sensor data into predictive models. The back-end makes inferences on this generated abstracted data. There are many ways to accomplish/solve these stages/components (Figure 3) (Cadena et al., 2016; Taheri & Xia, 2021).

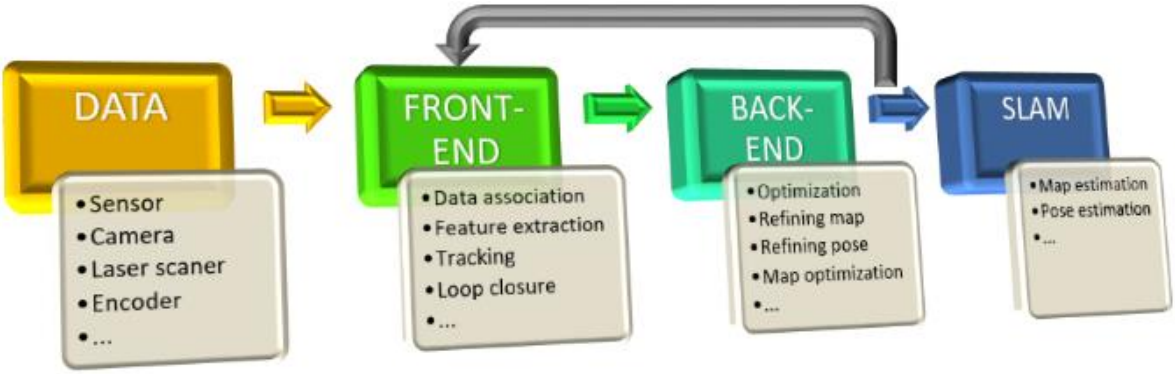

Figure 3. Typical SLAM architecture

2.1. Compared/used SLAM algorithms

2.1.1 LeGO-LOAM

Tixiao and Shan (2018) proposed LeGO-LOAM (Shan & Englot, 2018), a ground-optimized LiDAR SLAM algorithm that addresses the real-time estimation of six-degree-of-freedom poses for ground vehicles. This algorithm addresses key challenges and introduces novel strategies that enhance its performance.

The first notable contribution of LeGO-LOAM is in mitigating the impact of uneven terrain on point cloud motion distortion compensation, a common issue in LiDAR-based SLAM. It acknowledges noise introduced by ground-based point clouds, such as those originating from grass or leaves, as a primary factor contributing to misalignment of feature points. To compensate for this distortion, LeGO-LOAM incorporates a point cloud clustering and outlier rejection mechanism based on Breadth First Search (BFS). The second core innovation of LeGO-LOAM lies in the optimization of its front-end odometry computation. Recognizing the need for real-time performance, the algorithm divides the odometry estimation into two distinct steps. By breaking down the estimation of the pose variables into separate three-degree of freedom components, LeGO-LOAM reduces computation time. The initial step focuses on ground optimization, utilizing ground points to solve point-to-surface constraint problems for pitch, roll, and z-axis estimation. The subsequent step employs corner points, often extracted from multiline LiDAR scans, which predominantly represent vertical edge features. These corner points are leveraged to compute x, y, and yaw, thereby enhancing computational efficiency. This two-step approach not only accelerates the algorithm's processing but also contributes to its accuracy. The third critical advancement of LeGO-LOAM pertains to the utilization of key frames within the map construction process and the incorporation of the Graph-Based SLAM Library (GTSAM) for factor graph optimization. In the algorithm's back-end, key frames play a pivotal role in building a robust map representation. LeGO-LOAM employs GTSAM to optimize the factor graph, enhancing the accuracy of pose estimation and map reconstruction.

2.1.2 HDL-Graph SLAM

HDL-Graph SLAM (Koide et al., 2019) proposed in 2019 represents an advanced real-time Simultaneous Localization and Mapping (SLAM) algorithm tailored for 3D laser scanners, offering a comprehensive solution for robust trajectory estimation and environment mapping. This method is grounded in a 3D graph SLAM framework, bolstered by an innovative Normal Distributions Transform (NDT)-like scan matching procedure for precise trajectory determination. Notably versatile, HDL-Graph SLAM caters to six-degrees of freedom, facilitating accurate pose estimation across diverse spatial orientations.

A distinctive attribute of this algorithm is its capacity to seamlessly integrate additional sensor data, such as Inertial Measurement Unit (IMU) or Global Positioning System (GPS) inputs, as boundary conditions, thereby enriching trajectory refinement. At its core, HDL-Graph SLAM harnesses the power of Generalized Iterative Closest Point (GICP), a potent geometric registration technique capable of accommodating a range of geometric primitives, including points, line segments, and planes. This versatility stems from GICP's adeptness in representing geometry through a set of normal distributions, obviating the need for specialized functions for different primitive types. Notably, IMU data further enhances trajectory precision by cyclically aligning the IMU acceleration vector of each trajectory node with the gravity vector. Practical implementation involves a strategic down-sampling of the point cloud followed by iterative scan matching to estimate the sensor's pose, ensuring efficient and accurate localization within the 3D environment.

The basic comparison of used SLAM algorithms is given in Figure 4. Also, detailed explanations (theoretical information, mathematical background, etc.) are included in the relevant references (Shan & Englot, 2018; Koide et al., 2019; LeGO-LOAM, 2023; HDL-Graph SLAM, 2023).

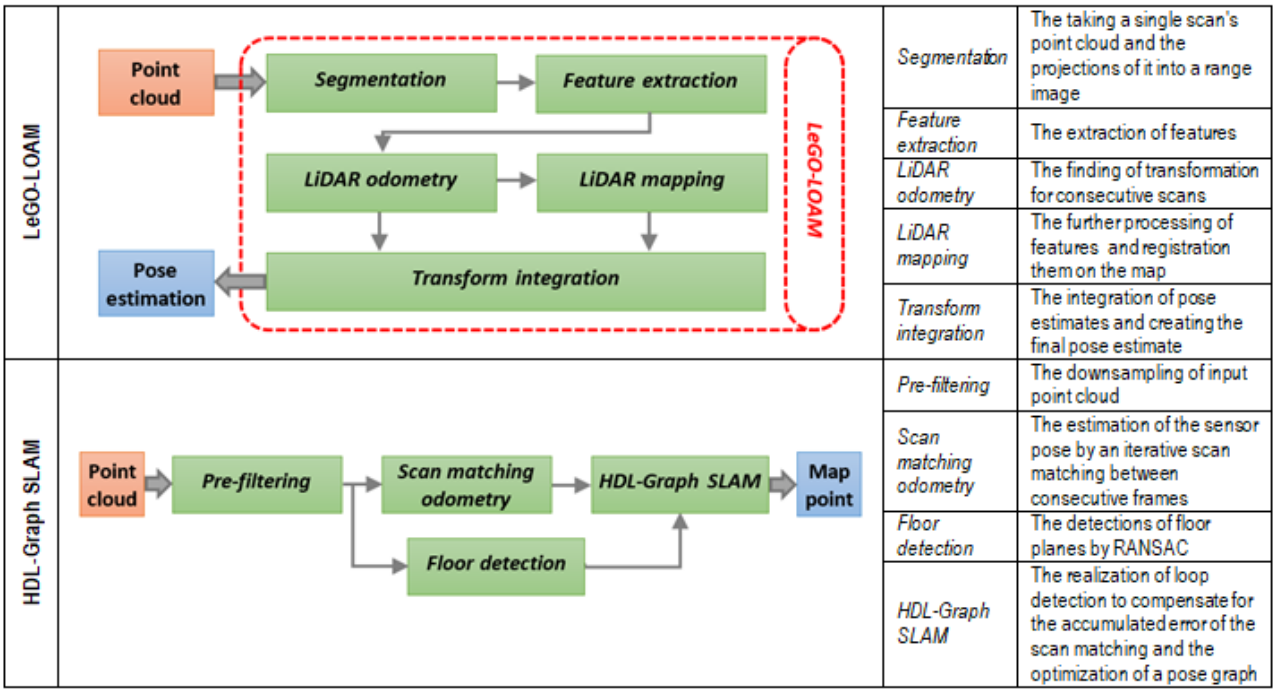

Segmentation	The taking a single scan's point cloud and the projections of it into a range image
Feature extraction	The extraction of features
LiDAR odometry	The finding of transformation for consecutive scans
LiDAR mapping	The further processing of features and registration them on the map
Transform integration	The integration of pose estimates and creating the final pose estimate
Pre-filtering	The downsampling of input point cloud
Scan matching odometry	The estimation of the sensor pose by an iterative scan matching between consecutive frames
Floor detection	The detections of floor planes by RANSAC
HDL-Graph SLAM	The realization of loop detection to compensate for the accumulated error of the scan matching and the optimization of a pose graph

Figure 4. The basic comparison of used SLAM algorithms

2.2 Error Metrics

Two widely adopted quantitative metrics, namely the Relative Pose Error (RPE) and the Absolute Trajectory Error (ATE), serve as crucial evaluative tools for comparing the performance of different algorithms in the context of trajectory estimation and localization. The ATE quantification involves the straightforward computation of the disparity between the estimated trajectory and the corresponding ground truth trajectory, post-alignment through a rigid body transformation denoted as S (Prokhorov et al., 2019):

$$F_i = Q_i^{-1} S P_i \tag{1}$$

Where P_i is the i^{th} estimated pose and Q_i is the corresponding ground truth pose. ATE is then calculated using is the root means squared over all these errors in the estimated trajectory:

$$ATE = \sqrt{\frac{1}{N}\sum_{i=1}^{N} trans(F_i)^2} \tag{2}$$

Where $trans(F_i)$ is the translation part of F_i. On the other hand, RPE facilitates a more nuanced assessment by investigating the evolution of localization discrepancies as the trajectory length expands. Calculated over trajectory segments, the relative pose error between the poses i and $i + 1$ is formulated as (Prokhorov et al., 2019):

$$F_i = (Q_i^{-1} Q_{i+1})^{-1} (P_i^{-1} P_{i+1}) \tag{3}$$

Analogous to ATE, the RPE metric is computed through the root mean squared method encompassing all time indices, thus encapsulating the trend of localization accuracy as trajectory length varies:

$$RPE = \sqrt{\frac{1}{N}\sum_{i=1}^{N} trans(F_i)^2} \tag{4}$$

3. Experimental Results

This section undertakes a comprehensive evaluation of the proposed HDL-Graph SLAM and LeGO-LOAM algorithms through the established ATE and RPE metrics as previously delineated. The evaluation is conducted on the widely recognized KITTI dataset

(Geiger et al., 2012), meticulously generated by the Karlsruhe Institute of Technology in Germany and the Toyota Institute of Technology in the USA, rendering it a pertinent and robust benchmark for algorithmic assessment. The dataset comprises point cloud data captured by the Velodyne HDL-64E LiDAR sensor, while its corresponding ground truth trajectory is established via the Oxford RT3000 inertial measurement unit (IMU). Specifically, this study harnesses sequences 01, 04, 05, 06, 07, 08, 09, and 10 from the KITTI benchmark for the evaluation. The ground truth trajectories pertaining to each sequence are visually depicted in Figure 5, affording a visual context for the subsequent analytical scrutiny.

In the instantiation of the Simultaneous SLAM algorithm using the KITTI dataset, the unprocessed data underwent a transformation into the rosbag format. This conversion facilitated the provision of input data to the SLAM algorithms under consideration. Subsequently, the resultant trajectories generated by the algorithms were systematically aggregated, and their congruence with the ground truth data from the KITTI dataset was meticulously examined to ascertain the incurred errors.

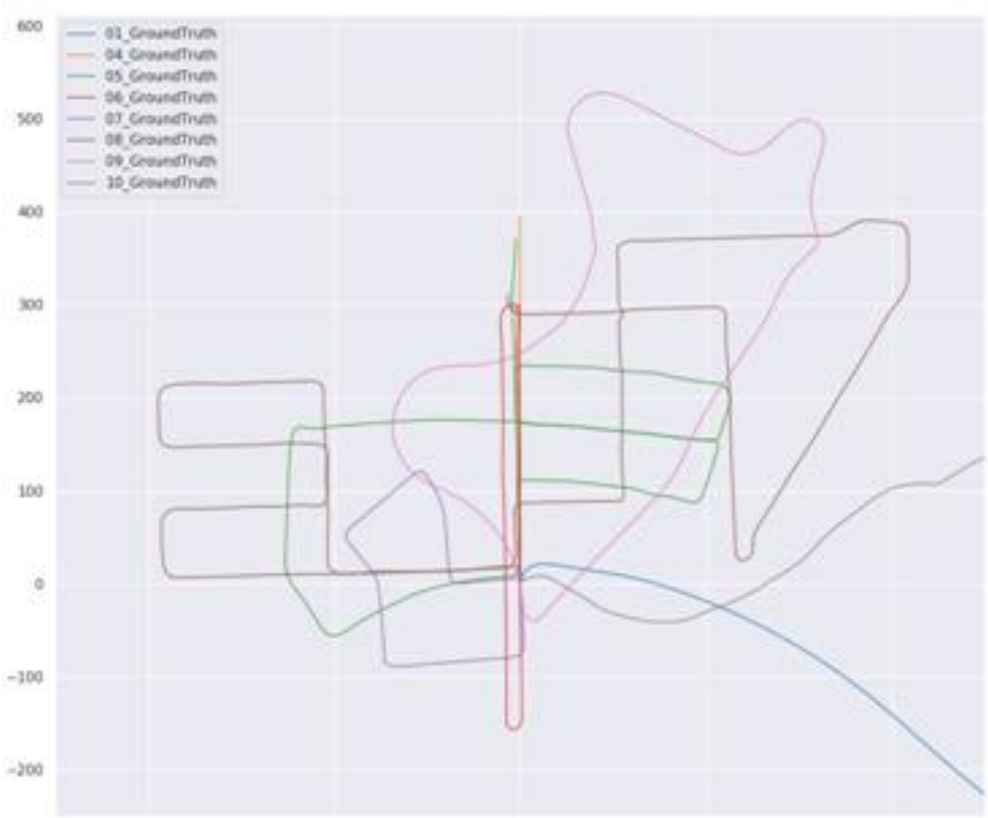

Figure 5. KITTI groud truth trajectories

The outcomes of the comparative analysis for the LeGO-LOAM and HDL-Graph SLAM algorithms, as presented in Tables 1 and 2 respectively, offer valuable insights into their respective performance on the KITTI dataset sequences (Figure 6).

Table 1. Results for LeGO-LOAM

LeGO-LOAM	ATE (m)	RPE (m)
01	1,6976	1,2028
04	0,4221	1,0352
05	3,0640	0,5844
06	0,6108	0,8001
07	3,0651	0,5943
08	1,6132	0,4141
09	3,0097	0,8997
10	3,0672	0,9048

In terms of ATE, it is evident that the HDL-Graph SLAM algorithm exhibits varying degrees of ATE across different sequences, with values ranging from 1.5643 m to 2.4175 m. Conversely, the LeGO-LOAM algorithm showcases a generally lower ATE, with values ranging from 0.4221 m to 3.0672 m. Notably, sequence 04 emerges as a particularly challenging instance for both algorithms in terms of ATE, warranting further investigation into the underlying factors contributing to this phenomenon.

Table 2. Results for HDL-Graph SLAM

HDL-Graph SLAM	ATE (m)	RPE (m)
01	2,4205	2,9071
04	1,5643	1,7782
05	2,0324	1,6206
06	1,9236	1,8882
07	2,1362	1,1997
08	2,4175	1,5167
09	2,0859	1,4549
10	2,3371	1,6678

Furthermore, the RPE analysis accentuates the algorithms' performance in terms of their ability to maintain accurate localization as trajectory length increases. Here, it is observed that the HDL-Graph SLAM algorithm exhibits RPE values spanning from 1.1997 m to 2.9071 m, reflecting varying degrees of pose estimation accuracy across the evaluated sequences. On the other hand, the LeGO-LOAM algorithm demonstrates generally lower RPE values, ranging from 0.4141 m to 1.2028 m. These results suggest that the LeGO-LOAM algorithm manifests a comparatively higher level of consistency in pose estimation accuracy across different trajectory lengths.

In conclusion, the analysis of ATE and RPE metrics underscores the nuanced performance characteristics of the HDL-Graph SLAM and LeGO-LOAM algorithms within the context of the KITTI dataset. While the HDL-Graph SLAM algorithm showcases versatility across sequences, the LeGO-LOAM algorithm exhibits a more uniform performance profile, particularly in maintaining pose estimation accuracy as trajectory length increases.

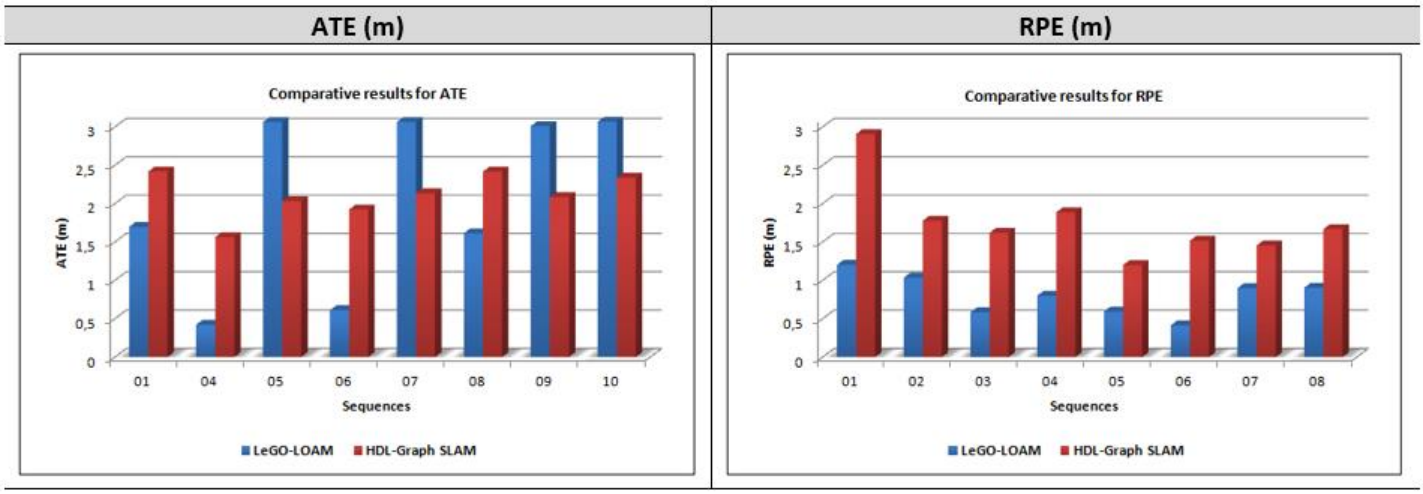

Figure 6. The comparative results for ATE and RPE

4. Conclusions

This study has conducted a comprehensive comparative analysis of two prominent LiDAR-based SLAM algorithms, namely HDL-Graph SLAM and LeGO-LOAM, using the KITTI dataset. By evaluating these algorithms through established metrics such as ATE and RPE, we have shed light on their distinctive performance characteristics, offering valuable insights for practitioners and researchers in the field of robotics and autonomous navigation.

First and foremost, our findings underscore the nuanced nature of algorithm performance. HDL-Graph SLAM exhibits versatility across different trajectory sequences, with fluctuations observed in both ATE and RPE values. This adaptability can be advantageous in scenarios where environmental conditions vary widely, showcasing its potential for use in diverse applications. Conversely, LeGO-LOAM demonstrates a more consistent performance profile, consistently displaying lower ATE and RPE values. This implies that LeGO-LOAM provides enhanced pose estimation stability, particularly as trajectory length increases. However, it's important to emphasize that the choice of algorithm should align with specific application requirements. HDL-Graph SLAM's adaptability may be preferred in situations where versatility is paramount, while LeGO-LOAM's consistent performance may be the choice for applications demanding higher accuracy and pose estimation stability.

In conclusion, our study contributes to the growing body of knowledge in the field of SLAM by providing a thorough comparative analysis of these two widely used LiDAR-based SLAM algorithms. We have demonstrated the importance of considering both ATE and RPE metrics in algorithm evaluation, as they reveal different facets of performance. Ultimately, the decision between HDL-Graph SLAM and LeGO-LOAM should be driven by the specific needs and constraints of the application at hand, and our findings

serve as a valuable reference for future research and practical implementations in the realm of autonomous navigation and robotics. As the field continues to evolve, further investigations and advancements are expected, and this work sets the stage for continued exploration and innovation in SLAM methodologies.

References

Cadena C., Carlone L., Carrillo H., Latif Y., Scaramuzza D., Neira J., Reid I., Leonard J. J. (2016). Past, present, and future of simultaneous localization and mapping: Toward the robust-perception age. IEEE Transactions on Robotics, 32(6), 1309-1332. doi: 10.1109/TRO.2016.2624754

Campos, C., Elvira, R., Rodríguez, J..J..G., Montiel, J..J..M., Tardós, J..D. (2021). ORB-SLAM3: An accurate open-source library for visual, visual–inertial, and multimap SLAM. IEEE Transactions on Robotics, 37(6), 1874-1890. doi: 10.1109/tro.2021.3075644

Cheng, J., Zhang, L., Chen, Q., Hu, X., Cai, J. (2022). A review of visual SLAM methods for autonomous driving vehicles. Engineering Applications of Artificial Intelligence, 114, 104992. doi: 10.1016/j.engappai.2022.104992

Dellaert, F., Kaess, M. (2006). Square Root SAM: Simultaneous localization and mapping via square root information smoothing. The International Journal of Robotics Research, 25(12), 1181-1203. doi: 10.1177/0278364906072768

Dissanayake, M. W. M. G., Newman, P., Clark, S., Durrant-Whyte, H. F., Csorba, M. (2001). A solution to the simultaneous localization and map building (SLAM) problem. IEEE Transactions on Robotics and Automation, 17(3), 229-241. doi: 10.1109/70.938381

Gao, B., Lang, H., Ren, J. (2020). Stereo visual SLAM for autonomous vehicles: A review. 2020 IEEE International Conference on Systems, Man, and Cybernetics (SMC), Toronto, ON, Canada, 11-14 October 2020, pp. 1316-1322. doi: 10.1109/SMC42975.2020.9283161

Geiger, A., Lenz, P., Urtasun, R. (2012). Are we ready for autonomous driving? The KITTI vision benchmark suite. 2012 IEEE Conference on Computer Vision and Pattern Recognition, Providence, RI, USA, 16-21 June 2012, pp. 3354-3361. doi: 10.1109/CVPR.2012.6248074

Guclu, O., Can, A. B. (2019) Fast and effective loop closure detection to improve SLAM performance. Journal of Intelligent & Robotic Systems, 93, 495-517. doi: 10.1007/s10846-017-0718-z

HDL-Graph SLAM, https://github.com/koide3/hdl_graph_slam, (2023)

Hoshi, M., Hara, Y., Nakamura, S. (2022). Graph-based SLAM using architectural floor plans without loop closure. Advanced Robotics, 36(15), 715-723. doi: 10.1080/01691864.2022.2081513

Huang, L. (2021). Review on LiDAR-based SLAM techniques. 2021 International Conference on Signal Processing and Machine Learning (CONF-SPML), Stanford, CA, USA, 14-14 November 2021, pp. 163-168. doi: 10.1109/CONF-SPML54095.2021.00040

Kaess, M., Johannsson, H., Roberts, R., Ila, V., Leonard, J., Dellaert, F. (2011). ISAM2: Incremental smoothing and mapping using the Bayes tree. Teh International Journal of Robotics Research, 31(2), 216-235. doi: 10.1177/0278364911430419

Kim, A., Eustice, R. M. (2013). Perception-driven navigation: Active visual SLAM for robotic area coverage. 2013 IEEE International Conference on Robotics and Automation, Karlsruhe, Germany, 06-10 May 2013, pp. 3196-3203. doi: 10.1109/ICRA.2013.6631022

Kim, B., Kaess, M., Fletcher, L., Leonard, J., Bachrach, A., Roy, N., Teller, S. (2010). Multiple relative pose graphs for robust cooperative mapping. 2010 IEEE International Conference on Robotics and Automation, Anchorage, AK, USA, 03-07 May 2010, pp. 3185-3192. doi: 10.1109/ROBOT.2010.5509154

Kim, C., Sakthivel, R., Chung, W..K. (2007). Unscented FastSLAM: A robust algorithm for the simultaneous localization and mapping problem. Proceedings 2007 IEEE International Conference on Robotics and Automation, Rome, Italy, 10-14 April 2007, pp. 2439-2445. doi: 10.1109/ROBOT.2007.363685

Kim, P., Chen, J., Cho, Y. K. (2018). SLAM-driven robotic mapping and registration of 3D point clouds. Automation in Construction, 89, 38-48. doi: 10.1016/j.autcon.2018.01.009

KITTI Dataset, http://www.cvlibs.net/datasets/kitti/evalodometry.php, (2023).

Koide, K., Miura, J., Menegatti, E. (2019). A portable three-dimensional LIDAR-based system for long-term and wide-area people behavior measurement. International Journal of Advanced Robotic Systems, 16(2). doi: 10.1177/1729881419841532

Kudriashov A., Buratowski T., Giergiel M., Małka P. (2020). SLAM techniques application for mobile robot in rough terrain. Mechanisms and Machine Science 87, Springer. doi: https://doi.org/10.1007/978-3-030-48981-6

LeGO-LOAM, https://github.com/RobustFieldAutonomyLab/LeGO-LOAM, (2023)

Leonard, J. J., Durrant-Whyte, H. F. (1991). Mobile robot localization by tracking geometric beacons. IEEE Transactions on Robotics and Automation, 7(3), 376-382. doi: 10.1109/70.88147

Makarenko A. A., Williams S. B., Bourgault F., Durrant-Whyte H. F. (2002). An experiment in integrated exploration. IEEE/RSJ International Conference on Intelligent Robots and Systems, Lausanne, Switzerland, 30 September - 4 October 2002, pp. 534-539. doi: 10.1109/IRDS.2002.1041445

Milford, M. J., Wyeth, G. F., Prasser, D. (2004). RatSLAM: a hippocampal model for simultaneous localization and mapping. IEEE International Conference on Robotics and Automation, 2004. Proceedings. ICRA '04., New Orleans, LA, USA, 26 April-01 May 2004, pp. 403-408. doi: 10.1109/ROBOT.2004.1307183

Montemerlo, M., Thrun, S., Koller, D., Wegbreit, B. (2002). FastSLAM: A factored solution to the simultaneous localization and mapping problem. Eighteenth National Conference on Artificial Intelligence, Edmonton Alberta, Canada, 28 July-1 August 2002, pp. 593-598

Moreno, L., Garrido, S., Blanco, D., Muñoz, M..L. (2009). Differential evolution solution to the SLAM problem. Robotics and Autonomous Systems, 57(4), 441-450. doi: 10.1016/j.robot.2008.05.005

Mur-Artal, R., Montiel, J..M..M., Tardós, J..D. (2015). ORB-SLAM: A versatile and accurate monocular SLAM system. IEEE Transactions on Robotics, 31(5), 1147-1163. doi: 10.1109/TRO.2015.2463671

Mur-Artal, R., Tardós, J..D. (2017). ORB-SLAM2: An open-source SLAM system for monocular, stereo, and RGB-D cameras. IEEE Transactions on Robotics, 33(5), 1255-1262. doi: 10.1109/TRO.2017.2705103

Niloy, M. A. K, Shama, A., Chakrabortty, R. K., Ryan, M. J., Badal, F. R., Tasneem, Z., Ahamed, M. H., Moyeen, S. I., Das, S. K., Ali, M. F., Islam, M. R., Saha, D. K. (2021). Critical design and control issues of indoor autonomous mobile robots: A review. IEEE Access, 9, 35338-35370. doi: 10.1109/ACCESS.2021.3062557

Prokhorov, D., Zhukov, D., Barinova, O., Anton, K., Vorontsova, A. (2019). Measuring robustness of Visual SLAM. 2019 16th International Conference on Machine Vision Applications (MVA), Tokyo, Japan, 27-31 May 2019, pp. 1-6. doi: 10.23919/MVA.2019.8758020

Shan, T., Englot, B. (2018). LeGO-LOAM: Lightweight and ground-optimized lidar odometry and mapping on variable terrain. 2018 IEEE/RSJ International Conference on Intelligent Robots and Systems (IROS), Madrid, Spain, 01-05 October 2018, pp. 4758-4765. doi: 10.1109/IROS.2018.8594299

Smith, R. C., Cheeseman, P. (1986). On the representation and estimation of spatial uncertainty. International Journal of Robotics Research, 5(4), 56-68. doi: 10.1177/027836498600500404

Sturm, J., Engelhard, N., Endres, F., Burgard, W., Cremers, D. (2012). A benchmark for the evaluation of RGB-D SLAM systems. 2012 IEEE/RSJ International Conference on Intelligent Robots and Systems, Vilamoura-Algarve, Portugal, 07-12 October 2012, pp. 573-580. doi: 10.1109/IROS.2012.6385773

Taheri H., Xia Z. C. (2021). SLAM; definition and evolution. Engineering Applications of Artificial Intelligence, 97, 104032. doi: 10.1016/j.engappai.2020.104032

Takleh, T. T. O., Bakar, N. A., Rahman, S. A., Hamzah, R., Aziz, Z. A. (2018). A brief survey on SLAM methods in autonomous vehicle. International Journal of Engineering&Technology, 7(4.27), 38-43. doi: 10.14419/ijet.v7i4.27.22477

Zhang J., Singh, S. (2014). LOAM: Lidar odometry and mapping in real-time. 2014 Robotics: Science and Systems Conference, University of California, Berkeley, USA, 12-16 July 2014, pp. 1-9. doi: 10.15607/rss.2014.x.007

Zhang, J., Singh, S. (2015). Visual-lidar odometry and mapping: low-drift, robust, and fast. 2015 IEEE International Conference on Robotics and Automation (ICRA), Seattle, WA, USA, 26-30 May 2015, pp. 2174-2181. doi: 10.1109/ICRA.2015.7139486

Zhang, L., Zhang, Y. (2022). Improved feature point extraction method of ORB-SLAM2 dense map. Assembly Automation, 42(4), 552-566. doi: 10.1108/AA-03-2022-0032